Am J Physiol Regul Integr Comp Physiol 307: R1146–R1156, 2014.
First published September 1, 2014; doi:10.1152/ajpregu.00513.2013.

Selective regulation of hepatic lipid metabolism by the AMP-activated protein kinase pathway in late-pregnant rats

Sandra C. Rodrigues,[1] Lucas C. Pantaleão,[1] Tatiane C. Nogueira,[1] Patrícia R. Gomes,[1] Gabriela G. Albuquerque,[2] Renato T. Nachbar,[1] Francisco L. Torres-Leal,[3] Luciana C. Caperuto,[4] Camilo Lellis-Santos,[5] Gabriel F. Anhê,[6] and Silvana Bordin[1]

[1]*Department of Physiology and Biophysics, Institute of Biomedical Sciences, University of São Paulo, São Paulo, Brazil;* [2]*School of Education, Sciences, Arts and Humanities, University of Grande Rio, Grande Rio, Brazil;* [3]*Department of Biophysics and Physiology, Health Science Center, Federal University of Piauí, Piauí, Brazil;* [4]*Department of Biological Sciences and* [5]*Institute of Environmental, Chemical and Pharmaceutical Sciences, Federal University of São Paulo, São Paulo, Brazil; and* [6]*Department of Pharmacology, Faculty of Medical Sciences, State University of Campinas, Campinas, Brazil*

Submitted 19 November 2013; accepted in final form 25 August 2014

Rodrigues SC, Pantaleão LC, Nogueira TC, Gomes PR, Albuquerque GG, Nachbar RT, Torres-Leal FL, Caperuto LC, Lellis-Santos C, Anhê GF, Bordin S. Selective regulation of hepatic lipid metabolism by the AMP-activated protein kinase pathway in late-pregnant rats. *Am J Physiol Regul Integr Comp Physiol* 307: R1146–R1156, 2014. First published September 1, 2014; doi:10.1152/ajpregu.00513.2013.—The liver plays an essential role in maternal metabolic adaptation during late pregnancy. With regard to lipid metabolism, increased secretion of very low-density lipoprotein (VLDL) is characteristic of late pregnancy. Despite this well-described metabolic plasticity, the molecular changes underlying the hepatic adaptation to pregnancy remain unclear. As AMPK is a key intracellular energy sensor, we investigated whether this protein assumes a causal role in the hepatic adaptation to pregnancy. Pregnant Wistar rats were treated with vehicle or AICAR (5-aminoimidazole-4-carboxamide ribonucleotide) for 5 days starting at *gestational day 14*. At the end of treatment, the rats were subjected to an intraperitoneal pyruvate tolerance test and in situ liver perfusion with pyruvate. The livers were processed for Western blot analysis, quantitative PCR, thin-layer chromatography, enzymatic activity, and glycogen content measurements. Blood biochemical profiles were also assessed. We found that AMPK and ACC phosphorylation were reduced in the livers of pregnant rats in parallel with a reduced level of hepatic gluconeogenesis of pyruvate. This effect was accompanied by both a reduction in the levels of hepatic triglycerides (TG) and an increase in circulating levels of TG. Treatment with AICAR restored hepatic levels of TG to those observed in nonpregnant rats. Additionally, AMPK activation reduced the upregulation of genes related to VLDL synthesis and secretion observed in the livers of pregnant rats. We conclude that the increased secretion of hepatic TG in late pregnancy is concurrent with a transcriptional profile that favors VLDL production. This transcriptional profile results from the reduction in hepatic AMPK activity.

pregnancy; liver; AMPK; lipid metabolism; very low-density lipoprotein

THE THIRD GESTATIONAL PERIOD is a physiological state of insulin resistance that, in normal pregnancies, lasts until the delivery (2, 13). Insulin resistance in glycolytic skeletal muscle fibers plays an important role in the reduced glucose clearance during pregnancy (33). However, the whole body maternal insulin resistance is compensated by an increase in β-cell mass and insulin secretion, which are also promptly reset after delivery (3, 11, 32, 44).

The nature of the metabolic changes associated with pregnancy that occur in the liver, including whether they are connected to hepatic insulin resistance, remains a matter of controversy. Some studies have reported that pregnancy is associated with an impairment of the insulin-induced suppression of hepatic glucose production (52) and reduced insulin receptor activation (40), whereas other works have reported increased hepatic insulin sensitivity mediated by the upregulation of tyrosine phosphorylation of insulin receptor substrate-1 in the liver (25). Moreover, in humans, there is a consensus that hepatic glucose production remains insulin-sensitive throughout normal pregnancy but is insulin-resistant in gestational diabetes (14, 19). In dogs, Connolly et al. (23) have demonstrated that the reduction in net hepatic glucose output is similar in pregnant and nonpregnant states, irrespective of using intermediate or high insulin doses.

As a key metabolic organ, the liver plays an integral role in energy homeostasis, not only by regulating glucose metabolism, but also by enhancing its production of triglycerides (TG) that return to the circulation as very low-density lipoproteins (VLDL) during lipid metabolism. Around parturition, the lipoprotein lipase in the mammary glands becomes active, which diverts circulating TG to this organ to ensure proper milk synthesis (28). Although the metabolic routes underlying this hepatic adaptation are well defined, the signaling pathways and transcriptional profile alterations that allow the liver to increase VLDL synthesis during pregnancy remain unspecified.

AMPK, a serine/threonine kinase, functions as a fuel sensor in several body tissues, including the liver. A growing body of evidence indicates that the regulatory role played by AMPK on hepatic metabolic fluxes correlates with hormone action in the liver, thus, suggesting that this enzyme may be a functional mediator of endocrine action during specific physiological states (26). Glucagon induces ACC phosphorylation and inactivation as a result of increased AMPK activity, which results in the suppression of lipid biogenesis (57).

Detailed studies have demonstrated the relevance of hepatic AMPK activity for the regulation of the metabolic demands during acute or chronic muscular work (15, 18) and fasting-

Address for reprint requests and other correspondence: S. Bordin, Dept. of Physiology and Biophysics, Institute of Biomedical Sciences, Univ. of São Paulo. Prof. Lineu Prestes Ave. #1524, São Paulo, Brazil 05508-000 (e-mail: sbordin@icb.usp.br).

refeeding conditions (5, 41); however, the involvement of hepatic AMPK in maternal lipid metabolism during pregnancy remains unexplored. In the present study, we aimed to evaluate the mechanisms involved in liver fuel metabolism during late pregnancy and focused on the AMPK-dependent regulation of lipid metabolism.

MATERIALS AND METHODS

Experimental design and animal treatment. Nulliparous Wistar rats at 8 wk of age were housed in a temperature-controlled room (22 ± 2°C) with the lights on from 7:00 AM to 7:00 PM; standard chow and water were available ad libitum. Rats were allowed to acclimate for 2 wk in our animal facility prior to being randomized into three groups: two groups were destined to breed and one remained nulliparous. Following habituation, two groups were housed with male rats for 5 days (two females and one male per cage). The concomitant presence of spermatozoa and estrous cells in a vaginal lavage indicated *day 0* of gestation. Pregnant rats were housed separately but remained in visual, olfactory, and auditory contact with unmated rats (i.e., nonpregnant) at all times.

Treatment with 5-aminoimidazole-4-carboxamide ribonucleotide (AICAR; cat. no. 2840; Tocris, Bristol, UK) consisted of a subcutaneous injection, 0.5 $mg \cdot kg^{-1} \cdot day^{-1}$ diluted in 0.9% NaCl, starting at *day 14* and continuing to *day 18* day of pregnancy. Two groups (pregnant and nonpregnant) received the same volume of vehicle during five consecutive days. Experiments were conducted on the day following the end of treatment. All studies were performed according to the guidelines of the Brazilian College for Animal Experimentation and approved by the Ethics Committee on Animal Use at the Institute of Biomedical Sciences, University of São Paulo, São Paulo, Brazil.

Blood sample analysis. Blood samples were collected at 9:00 AM. from nonfasting animals immediately after euthanasia and before the removal of liver samples. Glucose, TG, total cholesterol, and HDL cholesterol (HDL-C) concentrations were measured by colorimetric methods using commercial kits (Labtest Diagnostica, Minas Gerais, Brazil). Serum insulin (no. EZRMI-13K; Millipore, Billerica, MA) and portal plasma glucagon (cat. no. 297–57101, Wako Pure Chemical Industries, Osaka, Japan) concentrations were determined by ELISA, according to the respective manufacturer's instructions.

Glycogen content and liver-to-body weight ratio. Liver samples (~300 mg) from nonfasting animals were washed three times with ice-cold PBS and hydrolyzed with 2 ml of 30% KOH (1 h at 98°C). Glycogen was precipitated with 0.2 ml of Na_2SO_4 and 4.5 ml of 95% ethanol. Samples were then boiled for 15 s and centrifuged at 12,000 *g* for 15 min. The supernatant was discarded, after which, the pellet was diluted in warm distilled water. Samples were boiled again with 4.5 ml of 95% ethanol and centrifuged. Again, the supernatant was discarded, and the pellet was dissolved in warm distilled water. Glycogen concentration was measured with a colorimetric reaction by adding 1 ml of each sample, 15 μl of phenol solution (800 mg/ml), and 2 ml of H_2SO_4, and boiling for 15 min in a water bath. The absorbance was read at 490 nm.

Animals from each group were set apart to measure the liver-to-body weight ratio at the moment of euthanasia, i.e., the percentage of the liver to the body weight.

Maximal enzyme activity of de novo fatty acid synthesis. The activities of malic enzyme (EC 1.1.1.39) and glucose-6-phosphate dehydrogenase (G6PDH) (EC 1.1.1.49) were analyzed in liver and adipose tissue (subcutaneous and perigonadal depots) from nonfasting animals. For this analysis, liver and adipose tissue samples (~300 mg) were processed as previously described (21). Enzyme activities were expressed as nanomoles per minute per milligram of protein.

Intraperitoneal pyruvate tolerance test (ipPTT). Fasted rats (12 h) were anesthetized (sodium thiopental, 40 mg/kg) and subjected to an intraperitoneal injection containing sodium pyruvate solution (250 mg/ml) at a dosage of 2 g/kg. Glucose levels were determined in blood collected from the tail before (0 min) and 15, 30, 60, 90, and 120 min after an intraperitoneal pyruvate injection. The area under the curve (AUC) of glycemia vs. time was calculated using each individual baseline (basal glycemia) to estimate glucose production after a pyruvate load.

In situ liver perfusion with pyruvate. Fasted rats (12 h) were anesthetized and subjected to liver perfusion following the protocol described previously (24). In brief, rats were submitted to a laparotomy, and the livers were perfused with a warmed (37°C) and oxygenated perfusion buffer (Krebs-Henseleit bicarbonate buffer without glucose) via the portal vein. The effluent was collected by a cannula inserted into the infrahepatic segment of the cava vein. The perfusion was performed in an open system without recirculation of the perfusate. Livers were initially subjected to a preperfusion (20 min), followed by a 10-min perfusion when samples of the effluent fluid were collected at six different times (i.e., −10, −8, −6, −4, −2, and −1 min). Next, sodium pyruvate (5 mM) was added to the perfusion buffer, and the livers were perfused for an additional 40 min. During this interval, samples of the effluent perfusion fluid were collected at 0, 5, 10, 15, 20, 25, 30, 35, and 40 min after commencing the pyruvate perfusion.

Livers were removed and weighed after the perfusion period. The glucose concentration of the samples was measured (In Vitro Diagnostica Ltda, Distrito Industrial, MG, Brazil), and glucose production rates were expressed per liver mass ($\mu mol \cdot min^{-1} \cdot g^{-1}$) and plotted vs. time. The AUC during the perfusion with sodium pyruvate was

Table 1. *List of primer sets*

Gene	Forward primer (5′-3′)	Reverse primer (5′-3′)
apoB	CTGCGGTGGCAGAAATAACG	CCTTGAGCAAACCTTAGGTAGGG
cd36	TCTTCCAGCCAACGCCTTTGC	TGCACTTGCCAATGTCCAGCAC
dgat1	CAGACCAGCGTGGGCG	GAACAAAGAGTCTTGCAGACGATG
dgat2	AAGCCCATCACCACCGTTG	TTCCTTCCAGGAGCTGGCAC
fasn	TGGTGAAGCCCAGAGGGATC	CACTTCCACACCCATGAGCG
g6pc	ACCTTCTTCCTGTTTGGTTTCGC	CGGTACATGCTGGAGTTGAGGG
mttp	TATGACCGTTTCTCCAAGAGTGG	TCAAGGTTCTCCTCTCCCTCATC
pck1	AATGATGACCGTCTTGCTTTCG	TGGTCTGGACTTCTCTGCCAAG
sec22b	CGTGCTCGGAGAAATCTCGG	AACACGGCTACTGCTGCAAGC
stk11	AGCATGACCGTAGTGCCCTACC	GCCATTCACACAAACAGCCTTG
rpl37a	CAAGAAGGTCGGGATCGTCG	ACCAGGCAAGTCTCAGGAGGTG

Gene abbreviations and accession numbers are: apoB (NM_019287), apolipoprotein B; cd36 (AF072411), fatty acid translocase/CD36; dgat (NM_053437; NM_001012345), diacylglycerol O-acyltransferase; fasn (NM_017332), fatty acid synthase; g6pc (NM_013098), glucose-6-phosphatase, catalytic subunit; mttp (NM_001107727), microsomal triglyceride transfer protein; pck1 (NM_198780), phosphoenolpyruvate carboxykinase 1; sec22b (NM_001025686), vesicle trafficking protein homolog B; stk11 (NM_001108069), serine/threonine kinase 11/LKB1; rpl37a (X14069), ribosomal protein L37a.

calculated (μmol/g) to estimate the amount of glucose synthesized from pyruvate relative to the liver mass.

Protein extraction and immunoblotting. Anesthetized nonfasting rats were euthanized, and a fragment of the liver (~100 mg) was removed and processed for Western blot analysis, as previously described (45). The primary antibodies used were as follows: antiphosphorylated (p)AMPKα (Thr-172) (cat. no. 2535), anti-pACC (Ser-79) (cat. no. 3661), anti-pCREB (Ser-133) (cat. no. 9191), anti-CREB (cat. no. 9197), anti-pLKB1 (Ser-428) (cat. no. 3482), and anti-LKB1 (cat. no. 3047) from Cell Signaling Technology (Danvers, MA); anti-AMPKα-pan (cat. no. 07–181) and anti-ACC (cat. no. 04–322) from Millipore (Billerica, MA); and anti-glucose-6-phosphatase-α (sc-25840), anti-STAT3 (sc483), and anti-pSTAT3 (Tyr-705) (sc8059) from Santa Cruz Biotechnologies (Santa Cruz, CA). Anti-β-actin, acquired from Abcam (Cambridge, UK), was used as the loading control. Secondary antibodies conjugated to horseradish peroxidase (Bio-Rad Laboratories, Hercules, CA) were used, followed by chemiluminescent detection of the bands on X-ray-sensitive films. Optical densitometry of the films was performed using the Scion Image analysis software (Scion, Frederick, MD).

RNA extraction and qPCR. Total RNA was extracted from samples of liver tissue (~100 mg) collected from nonfasting animals using TRIzol reagent, as previously described (45). Extracted RNA was eluted in RNase-free water, treated with Turbo DNA-free (Ambion, Austin, TX), according to the manufacturer's specifications and quantified by spectrophotometry at 260 nm with acceptable 260/280 nm ratios between 1.8 and 2.0. RNA quality was assessed by ethidium bromide agarose gel electrophoresis.

For mRNA expression analysis, 1 μg of total RNA was reverse transcribed using Improm-II reverse transcriptase (Promega, Madison, WI) and random primers, according to the manufacturer's instructions. Real-time amplifications were performed using Kapa SYBR fast DNA polymerase (Kapa Biosystems, Woburn, MA) and following standard procedures. Values of mRNA expression were normalized to the internal control gene *rpl37a* using the $\Delta\Delta C_T$ method. Primer sequences are in Table 1.

Lipid extraction and thin-layer chromatography. The hepatic lipid content of nonfasting animals was determined according to methods described elsewhere (54). Briefly, each sample (~200 mg) was homogenized in methanol:chloroform:PBS solution (1:2:1, vol/vol) and centrifuged at 15,000 *g* for 1 min. The upper phase was removed and reextracted with PBS:chloroform:methanol solution (0.8:1:1, vol/vol). The lower phase was then reextracted with Folch solution (chloroform:methanol:water, 3:47:48, vol/vol), and the organic phase containing the lipid extract was dried (Speed Vac, Savant). The tubes were frozen with liquid nitrogen and stored at −20°C until chromatographical analysis.

Dried samples were chromatographed using thin-layer chromatography with a 250-mm stationary phase of silica gel 60 H and a solvent system consisting of hexane:diethylic ether:acetic acid (70:30:1, vol/vol) at 26 ± 2°C. The samples were developed in chloroform:methanol:water:ammonium hydroxide (25%) (120:75:6:2, vol/vol), and the plates were visualized in an atmosphere of iodine vapor prior to scanning and densitometry.

Statistical analysis. All results are presented as the means ± SE. Comparisons were performed using an unpaired Student's *t*-test or a one-way ANOVA, followed by a Tukey-Kramer post hoc testing when appropriate (INStat, GraphPad Software, San Diego, CA). *P* values <0.05 indicate a significant difference.

RESULTS

Maternal hepatic gluconeogenesis is reduced at the end of pregnancy. We initially assessed changes in glucose clearance after in vivo challenge with pyruvate (pyruvate tolerance test) as an indicator of gluconeogenesis modulation during pregnancy. The changes in glucose levels over time after a challenge with exogenous pyruvate revealed lower mean glucose levels in pregnant rats when compared with nonpregnant rats. Significantly lower glucose levels were found at 60, 90, and 120 min after pyruvate challenge. Thus, the AUC obtained from the curve was reduced in pregnant rats (43% of that in nonpregnant rats; $P < 0.05$) (Fig. 1*A*).

We next assessed hepatic gluconeogenesis to determine whether the increased glucose clearance after a pyruvate load during pregnancy was due to the reduced hepatic conversion of pyruvate into glucose. An in situ liver perfusion showed that

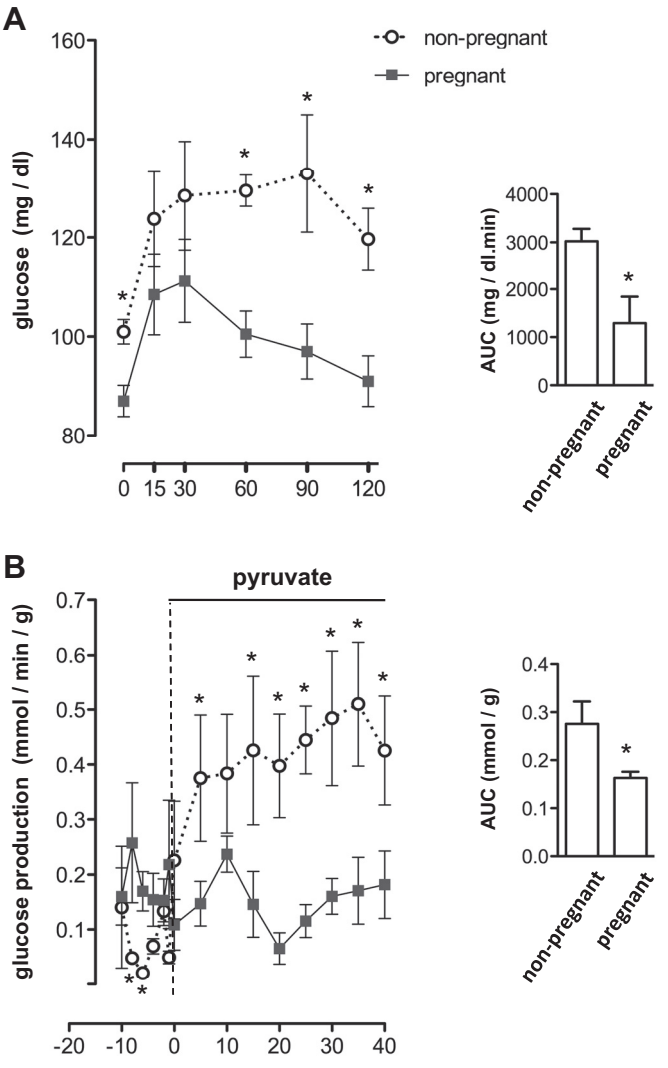

Fig. 1. Hepatic gluconeogenesis after pyruvate load is reduced in late-pregnant rats. Pregnant (*gestational day 19*) and nonpregnant rats were subjected to an intraperitoneal pyruvate tolerance test. Glycemia was measured before and 15, 30, 60, 90, and 120 min after sodium pyruvate injection. The area under the curve (AUC) was calculated for each individual animal within each group (*A*). Pregnant and nonpregnant rats were subjected to in situ liver perfusion with sodium pyruvate. Glucose levels in the perfusate were quantified before (−10, −8, −6, −4, −2, −1, and 0 min) and after (5, 10, 15, 20, 25, 30, 35, and 40 min) sodium pyruvate addition to the perfusion buffer. The glucose production rate was expressed per liver mass ($\mu mol \cdot min^{-1} \cdot g^{-1}$) and plotted vs. time. The AUC during the perfusion with sodium pyruvate was calculated (μmol/g) to estimate the amount of glucose synthesized from pyruvate relative to the liver mass (*B*). The results are shown as the means ± SE. *$P < 0.05$ vs. nonpregnant group ($n = 4$).

the livers of pregnant rats exhibited reduced rates of glucose synthesis throughout the period in which pyruvate was present in the perfusion medium. This result was best observed between 20 and 30 min after the beginning of perfusion with pyruvate. The total mass of glucose synthesized from pyruvate relative to liver weight was also lower in pregnant rats (59% of that in nonpregnant rats; $P < 0.05$) (Fig. 1*B*).

Changes in hepatic cellular signaling at the end of pregnancy. The blood glucagon-insulin ratio was assessed in nonpregnant and late-pregnant rats. As expected, the insulin levels of pregnant rats were higher than those in nonpregnant control rats (2.74 ± 0.47 ng/ml vs. 0.85 ± 0.13 ng/ml, respectively; $P < 0.05$), and the glucagon levels were unchanged (1.63 ± 0.08 ng/ml and 1.75 ± 0.10 ng/ml, respectively). Thus, at this stage of pregnancy, the glucagon-insulin ratio was significantly decreased in pregnant rats (33% of that in nonpregnant rats; $P < 0.05$) (Fig. 2*A*).

The cAMP response element binding protein (CREB) is a transcriptional factor activated by glucagon via PKA-mediated phosphorylation. In agreement with the glucagon-insulin ratio, our results showed that CREB phosphorylation was 44% lower in the livers of pregnant rats than that in the nonpregnant rats ($P < 0.05$; Fig. 2*B*).

On the other hand, we found increased STAT3 tyrosine phosphorylation in the livers of pregnant rats (46% higher than that in nonpregnant rats; $P < 0.05$) (Fig. 2*C*). STAT3 is a transcription factor that was previously described to bind to *g6pc* genes, thereby repressing their transcription (49). *G6pc* expression and G6Pase content were reduced in the livers of pregnant rats (66% and 35% lower, respectively, than nonpregnant rats; $P < 0.05$) (Fig. 2, *D* and *E*).

Reduced activity of the AMPK signaling pathway in the livers of pregnant rats. The AMPKα content was not significantly altered in the livers of pregnant rats, irrespective of treatment with AICAR (Fig. 3*A*). AMPKα phosphorylation was reduced in the livers of pregnant rats (25% lower than in nonpregnant rats; $P < 0.05$). Treatment with AICAR restored AMPKα phosphorylation levels in the livers of pregnant rats to values similar to those of nonpregnant rats (Fig. 3*B*). The expression of ACC, a downstream target of AMPKα, was not altered in the livers of pregnant rats or pregnant rats treated with AICAR (Fig. 3*C*). Similar to AMPKα phosphorylation, ACC phosphorylation was reduced in the livers of pregnant rats (41% lower than in nonpregnant rats; $P < 0.05$). Treatment with AICAR restored ACC phosphorylation levels in the livers

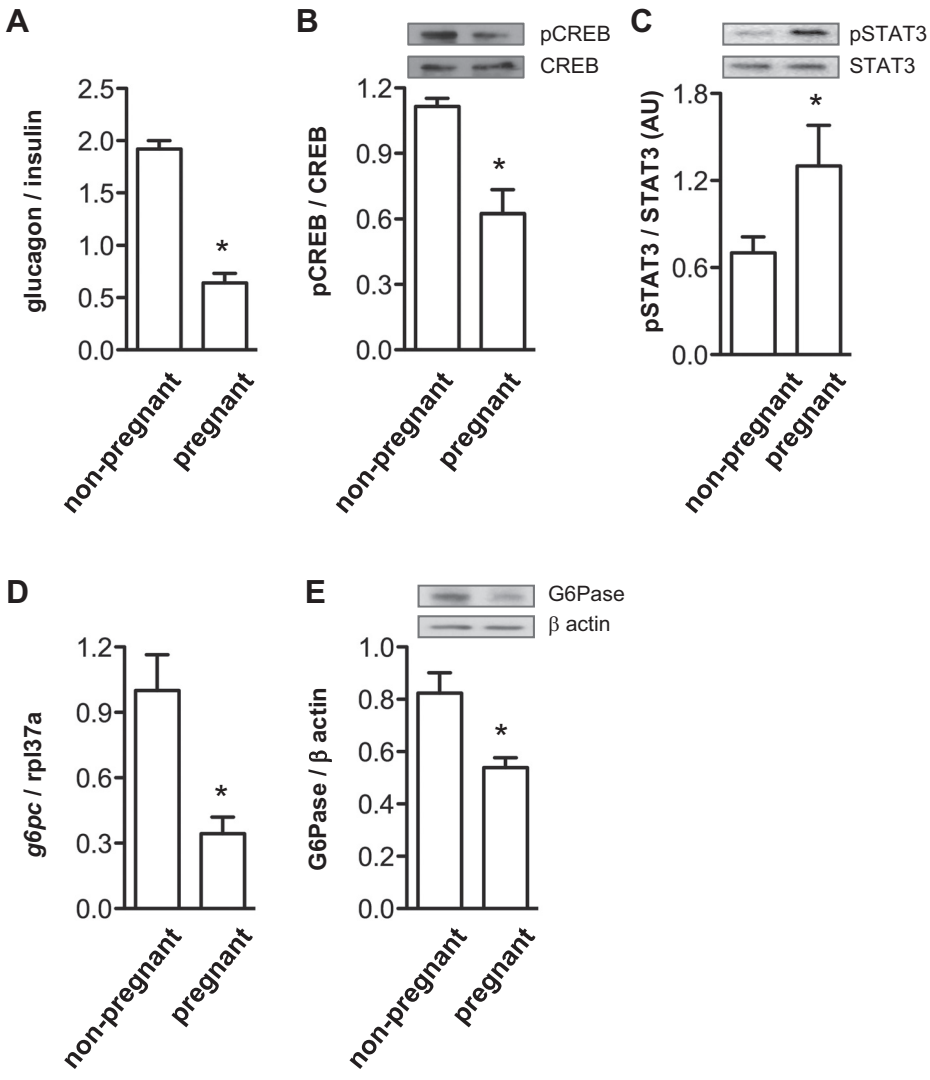

Fig. 2. Liver glucagon and STAT3 signaling correlates with G6Pase expression and gluconeogenesis in late pregnancy. Blood glucagon and insulin levels from pregnant (*gestational day 19*) and nonpregnant rats were measured to calculate the glucagon/insulin ratio (*A*). Phosphorylated CREB (*B*) and STAT3 (*C*) were analyzed by immunoblotting liver samples obtained from pregnant and nonpregnant rats. Phosphorylated CREB and STAT3 were normalized by their respective protein contents. These samples were also used for the analysis of the mRNA expression of *g6pc* (*D*) and the protein content of G6Pase by immunoblotting (*E*). G6Pase protein content was normalized by β-actin protein content. The results are shown as the means ± SE. *$P < 0.05$ vs. nonpregnant rats ($n = 4$ to 11).

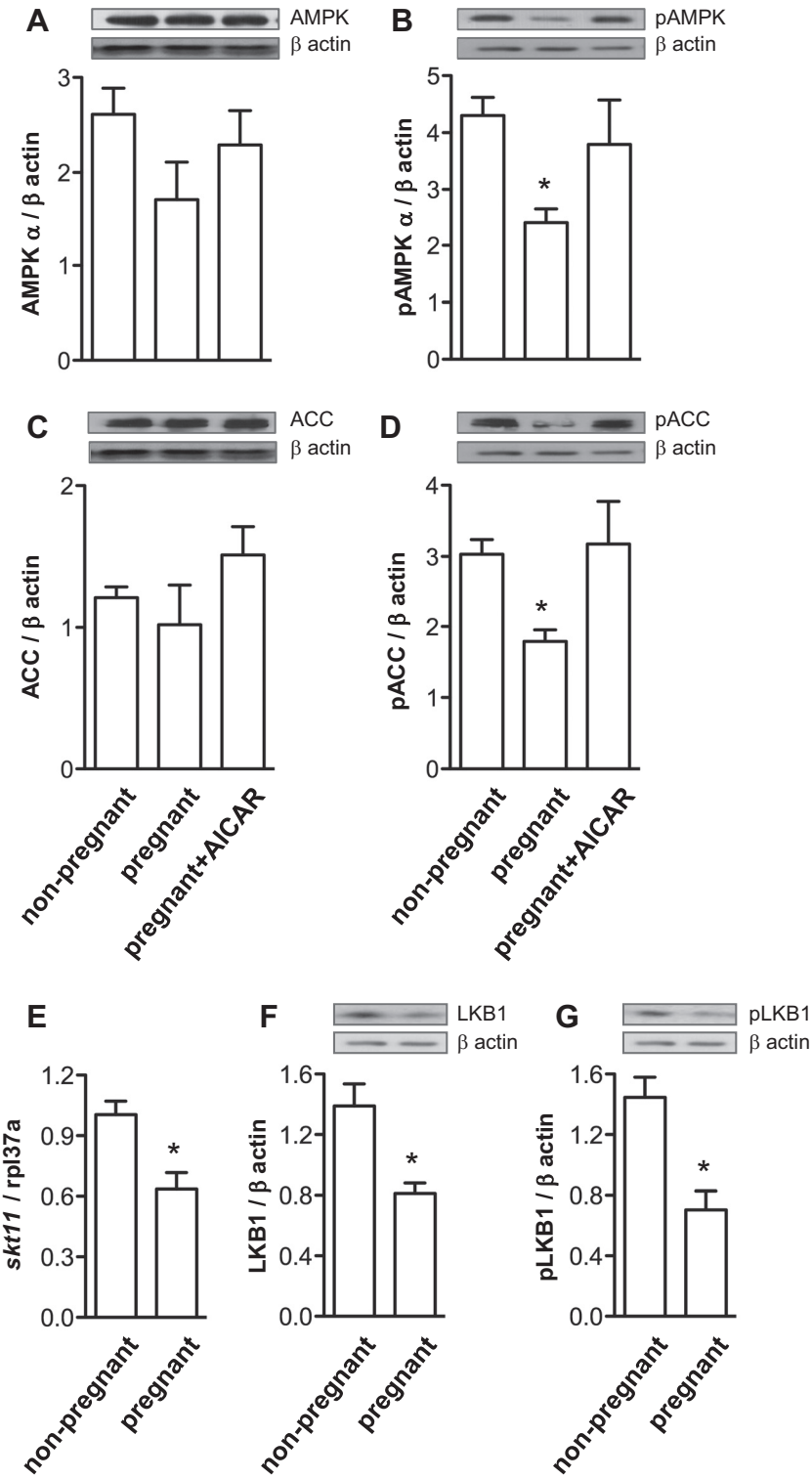

Fig. 3. The AMPK pathway is down-regulated in the livers of late-pregnant rats. Liver samples, both from pregnant (*gestational day 19*) rats with or without 5-aminoimidazole-4-carboxamide ribonucleotide (AICAR) treatment and from age-paired nonpregnant rats, were processed for Western blot detection of AMPK (*A*), phosphorylated AMPK (*B*), acetyl-CoA carboxylase (ACC; *C*), and phosphorylated ACC (*D*). Samples from nonpregnant and untreated pregnant rats were also used for Western blot detection of liver kinase B1 (LKB1) (*F*) and phosphorylated LKB1 (*G*), and for RNA extraction and qPCR analysis of the gene that encodes LKB1, *stk11* (*E*). Immunoblots were normalized by β-actin protein content. The results are shown as means ± SE. *$P < 0.05$ vs. nonpregnant and pregnant+AICAR groups ($n = 6$ to 14).

of pregnant rats to values similar to those of nonpregnant rats (Fig. 3*D*).

LKB1, an upstream activator of AMPK, was reduced in the livers of pregnant rats at both the mRNA and protein levels (37% and 42% lower, respectively, than that in nonpregnant rats; $P < 0.05$) (Fig. 3, *E* and *F*); the level of LKB1 phosphorylation was also reduced in pregnant rats (51% lower than that in nonpregnant rats; $P < 0.05$) (Fig. 3*G*).

Biochemical profile of pregnant rats treated with AICAR. Random glycemia was reduced in pregnant rats (18% lower than that in nonpregnant rats; $P < 0.05$), and this reduction was abolished by treatment with AICAR (Fig. 4*A*). Circulating TG were increased in pregnant rats irrespective of AICAR treatment (98% and 84% higher, respectively, than in nonpregnant rats; $P < 0.05$) (Fig. 4*B*). The total circulating cholesterol and HDL-C levels were similar among

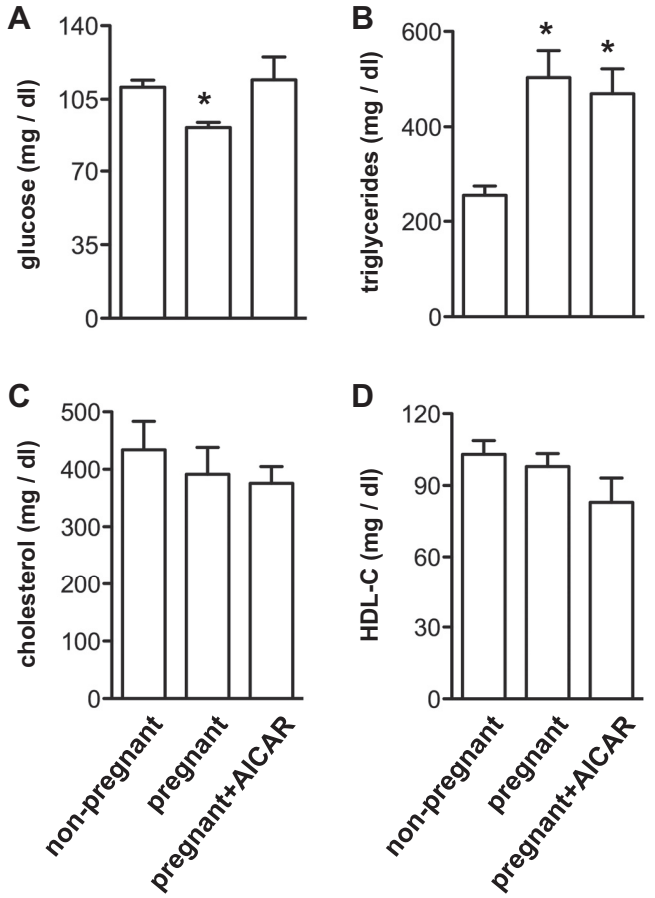

Fig. 4. Blood biochemical profile and glycogen content of nonpregnant rats, untreated pregnant rats, and pregnant rats treated with AICAR. Blood samples were used to measure circulating glucose (*A*), triglycerides (TG; *B*), cholesterol (*C*), and HDL-cholesterol (*D*). Experiments were conducted on *gestational day 19*. The results are shown as the means ± SE. *$P < 0.05$ vs. nonpregnant and pregnant+AICAR rats ($n = 5$ to 12).

nonpregnant, pregnant, and pregnant+AICAR rats (Fig. 4, *C* and *D*, respectively).

Changes in hepatic TG and glycogen content during pregnancy are modulated by AICAR. The hepatic content of phospholipids, free cholesterol, cholesterol esters, and free fatty acids were similar among nonpregnant, pregnant and pregnant+AICAR rats (Figs. 5, *A–D*). However, we found a reduction in hepatic TG in pregnant rats (19% lower than in nonpregnant rats; $P < 0.05$) that was blunted by AICAR treatment (Fig. 5*E*).

The reduction in hepatic glycogen content observed in pregnant rats (48% lower than in nonpregnant rats; $P < 0.05$) was suppressed by AICAR treatment. Conversely, the increased body and liver weight and liver-to-body weight ratio in pregnant rats (43%, 70%, and 20% higher, respectively, than in nonpregnant rats; $P < 0.05$) were not changed by AICAR (Table 2).

Malic enzyme activity of pregnant rats is regulated by AICAR in the liver but not in adipose tissue. Malic enzyme activity was increased in the liver and in perigonadal and subcutaneous adipose tissue of pregnant rats (28%, 253%, and 263% higher, respectively, than in nonpregnant rats; $P < 0.05$). Treatment with AICAR restored malic enzyme activity in the livers of pregnant rats to values similar to those found in nonpregnant rats. The malic enzyme activity of adipose tissue from pregnant rats was not affected by AICAR treatment (Fig. 6*A*). Hepatic G6PDH activity in both pregnant and pregnant+AICAR rats was similar to that in nonpregnant rats. Pregnancy was associated with an increase in G6PDH activity in both perigonadal and subcutaneous adipose tissue (60% and 44% higher, respectively, than in nonpregnant rats; $P < 0.05$), which was unaffected by AICAR treatment (Fig. 6*B*). Of note, differences in malic enzyme and G6PDH activity in the livers of late-pregnant rats have been described previously (43).

Expression profile of genes related to lipid metabolism in the livers of pregnant rats treated with AICAR. Previous research has demonstrated that hepatic de novo lipogenesis and VLDL-TG synthesis are increased in late pregnancy, whereas hepatic TG content is decreased (29, 37). To investigate the transcriptional profile underlying the reversal of the hepatic TG content in pregnant rats following AICAR treatment, we searched for changes in the expression of genes related to TG synthesis and VLDL assembly (Fig. 7). The expression of *fasn*, the gene that encodes fatty acid synthase, was upregulated in late pregnancy (97% increase compared with nonpregnant rats; $P < 0.05$) and was restored by AICAR treatment. Additionally, *dgat1* and *dgat2* (which encode the two *O*-acyltransferase isozymes) expression was increased in the livers of pregnant rats (86% and 163% higher, respectively, than in nonpregnant rats; $P < 0.05$), and was also restored by AICAR treatment.

The expression of the gene encoding the microsomal triglyceride transfer protein (*mttp*) was not altered either by the pregnant state or by AICAR treatment. However, fatty acid translocase (*cd36*) gene expression was upregulated both by pregnancy (331%; $P < 0.05$) and by AICAR treatment. In the livers of pregnant rats treated with AICAR, *cd36* expression increased by an additional 68% ($P < 0.05$). The expression of the vesicle-trafficking protein SEC22b (*sec22b*) was also regulated by the pregnant state; *sec22b* expression was significantly elevated in livers from untreated pregnant rats when compared with the other two groups (270% higher than in nonpregnant rats; $P < 0.05$). Moreover, AICAR treatment abolished the *sec22b* overexpression in pregnancy. Finally, we analyzed the expression of *apoB*, the gene that encodes the rat apolipoprotein B. We found that pregnancy upregulated *apoB* expression (338% higher than the nonpregnant values; $P < 0.05$) and that AICAR treatment restored *apoB* levels to values similar to those observed in nonpregnant rats.

Pck1, the gene that encodes PEPCK, was evaluated as a control of AICAR treatment (36). As expected, AICAR reduced *pck1* expression (to 43% of that in pregnant rats; $P < 0.05$).

DISCUSSION

Pieces of evidence point to a physiological regulation of hepatic AMPK activity in response to changes in the circulating levels of various hormones (6, 7, 8, 15, 18, 60). For example, the fasting- or physical exercise-induced increase of the glucagon-insulin ratio causes AMPK activation in the liver (7, 8, 18, 41). Overwhelming glucagon signaling promotes hepatic glucose production and inhibits lipid biogenesis (reviewed in Ref. 26). Our present data show that maternal liver

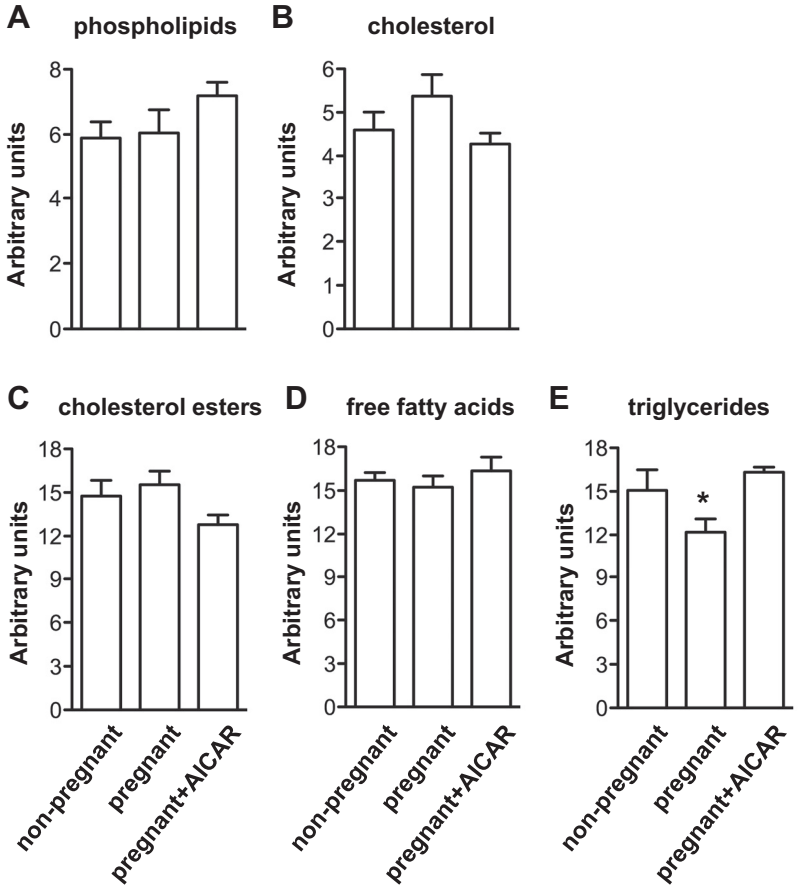

Fig. 5. Hepatic lipid profile of nonpregnant rats, untreated pregnant rats, and pregnant rats treated with AICAR. Lipids were extracted and subjected to thin-layer chromatography. The plates were scanned to evaluate the hepatic content of phospholipids (*A*), cholesterol (*B*), cholesterol esters (*C*), free fatty acids (*D*), and TG (*E*). The values were expressed as arbitrary units. Experiments were conducted on *gestational day 19*. The results are shown as the means ± SE. *$P < 0.05$ vs. nonpregnant and pregnant+AICAR rats ($n = 5$ to 10).

metabolism responds as expected to the reduced glucagon-insulin ratio as follows: *1*) decreased hepatic glucose production after pyruvate load; *2*) decreased AMPK activation; and *3*) increased de novo lipogenesis. Moreover, we provide several additional pieces of evidence to support the hypothesis that the AMPK pathway has a central role in the regulation of hepatic energy metabolism during pregnancy.

In addition to the reduced glucagon-insulin ratio, other pregnancy-related endocrine factors are theoretically able to contribute to the hepatic adaptation to pregnancy. Estrogens, for example, have been shown to reduce hepatic TG accumulation in nonpregnant rodents, but the activation of estrogen receptors was suggested to positively regulate AMPK activity (59, 22). Moreover, in premenopausal women, the menstrual cycle phase alone does not affect circulating TG or plasma apoB100 (39). Thus, the isolated actions of sex steroids are unlikely to completely account for the adaptation described herein.

Table 2. *Body and liver weights, liver-to-body weight, and hepatic glycogen content in nonpregnant, pregnant, and pregnant+AICAR rats*

	Nonpregnant	Pregnant	Pregnant+AICAR
Body weight, g	245.3 ± 8.7 (4)	350.7 ± 9.9* (4)	376.7 ± 6.8* (4)
Liver weight, g	7.4 ± 0.1 (4)	12.6 ± 0.2* (4)	14.7 ± 0.7* (4)
Liver-to-body weight ratio	3.0 ± 0.2 (4)	3.6 ± 0.1* (4)	3.9 ± 0.2* (4)
Hepatic glycogen, %	2.2 ± 0.2 (10)	1.2 ± 0.1*# (8)	2.0 ± 0.1 (5)

Nonpregnant, pregnant and pregnant+AICAR rats were weighed and euthanized. Livers were collected, weighted, and processed for glycogen determination. Data are presented as the means ± SE (*n*). *$P < 0.05$ vs. nonpregnant; #$P < 0.05$ vs. pregnant+AICAR.

As STAT3 was described to bind to and repress the transcription of *g6pc* (49), the increased STAT3 phosphorylation in the liver during pregnancy might explain the decrease in G6Pase expression. A myriad of signaling pathways, including IL-6, IL-22, leptin, and growth hormone signaling, could activate STAT3 in the liver (10, 50, 58). Among them, leptin is increased during pregnancy and, by extension, is a putative candidate to participate in this effect (5, 34). Also, considering that the phosphorylation of CREB is a key step through which glucagon stimulates G6Pase expression (53), we cannot rule out that the decreased levels of pCREB might also contribute to the reduced gluconeogenesis in the liver of pregnant rats. Moreover, it has been recently demonstrated that the activation of AMPK inhibited STAT3 phosphorylation in both murine hepatocytes and HepG2 cell line (17, 35, 42), indicating that the increase in STAT3 phosphorylation found in the liver of late-pregnant rats could be due to the reduced AMPK activation.

The activity of AMPK is regulated by direct allosteric activation, as well as the reversible phosphorylation of Thr-172 within the catalytic subunit by at least the following two upstream kinases: *1*) the tumor suppressor LKB1/SKT11 (serine/threonine kinase-11) and *2*) CaMKKβ (Ca^{2+}/calmodulin-dependent protein kinase kinase-β). In the liver, LKB1 plays a crucial role in activating AMPK and in controlling glucose and

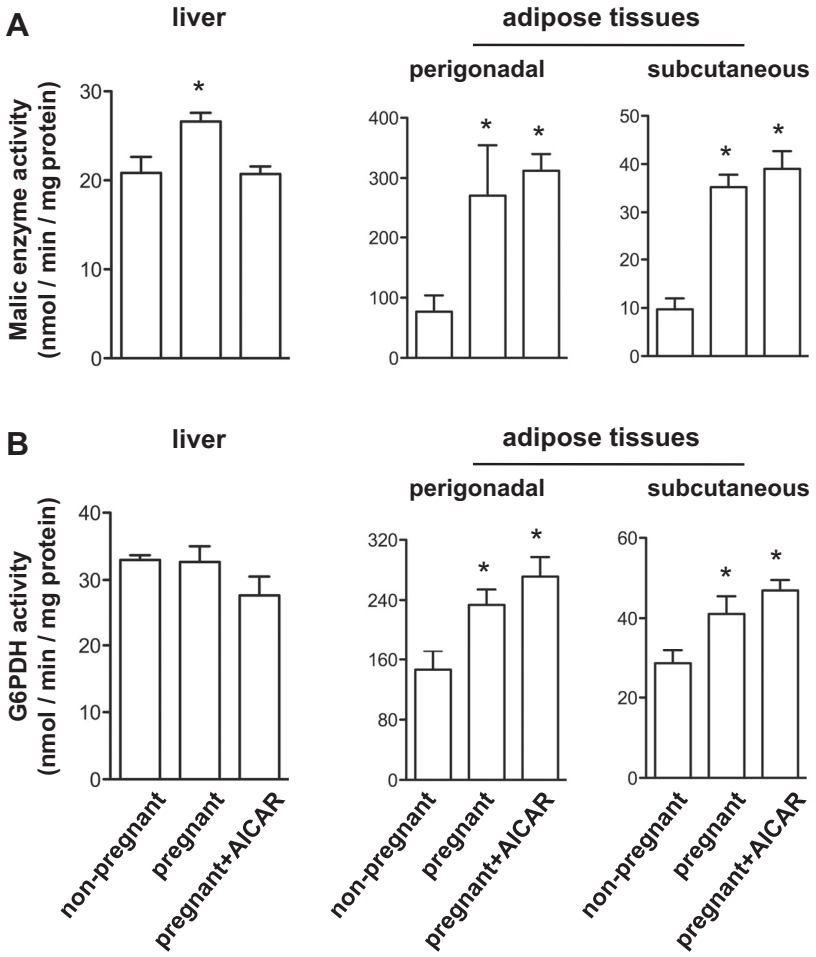

Fig. 6. Activity of enzymes related to the lipogenic pathway in the liver and adipose tissue of nonpregnant and pregnant rats treated or not with AICAR. Fragments of the liver and the perigonadal and subcutaneous adipose tissue were removed and processed for malic enzyme (*A*) and G6PDH (*B*) activities. Experiments were conducted on *gestational day 19*. The results are shown as the means ± SE. *$P < 0.05$ vs. nonpregnant rats ($n = 4$ to 6).

lipid metabolism (30, 55). Accordingly, our data show that LKB1 expression and phosphorylation, as well as its downstream target AMPK, were downregulated in the livers of late-pregnant rats. Moreover, the phosphorylation of ACC, a rate-limiting enzyme of fatty acid synthesis that is phosphorylated and inactivated by AMPK (27), was also reduced, which suggests a redirection of the pyruvate flux to the lipogenic rather than the gluconeogenic metabolic pathway. Evidence for this theory is given by the data from the hepatic perfusion with pyruvate and the pyruvate tolerance test.

Additionally, the upregulation of malic enzyme activity reported herein suggests increased hepatic synthesis of TG during pregnancy. Malic enzyme is a key lipogenic enzyme that catalyzes malate decarboxylation and generates NADPH to de novo fatty acid synthesis by FASN (1). Thus, we hypothesize that the depletion of hepatic TG content observed in pregnant rats is due to the increased VLDL secretion rather than the reduced de novo synthesis of fatty acids. Our data also suggest that this hepatic adaptation to pregnancy, which is characterized by increased fatty acid synthesis and VLDL secretion, is dependent upon the downregulation of AMPK in the liver, given that AICAR treatment normalizes hepatic malic enzyme activity and TG content. We cannot, however, exclude the participation of additional signaling pathways in this adaptation since AICAR is not a highly specific AMPK activator.

Maternal hypertriglyceridemia, which is one of the most striking physiological changes to occur in late pregnancy, favors the use of lipids by key maternal tissues and is likely to contribute to glucose sparing for fetal accretion. When compared with virgin rats, a higher rate of maternal de novo liver lipogenesis was observed at the 20th day of pregnancy (37). Importantly, pregnancy-related hypertriglyceridemia is a consequence of both the increase in hepatic VLDL production and the reduced TG removal from the bloodstream due to the downregulation of lipoprotein lipase activity in adipose and muscle tissues (29). This fact most likely explains why AMPK activation with AICAR restores hepatic TG without affecting the levels of circulating TG. As we understand, the reduced TG removal from the bloodstream during pregnancy acts as the limiting step that determines fluctuations in circulating lipids. In accordance with this hypothesis, it is noteworthy that adipose tissue lipoprotein lipase activity is insensitive to AICAR-induced AMPK activation (46). Notably, the rats that were used for biochemical measurements were under nonfasting conditions. Therefore, intestinal chylomicron production needs to be considered as a relevant source of circulating TG.

Our data indicating that the increased levels of malic enzyme activity in the adipose tissue of pregnant rats are not affected by AICAR further suggests that AMPK plays a specific role in the energy metabolism adaptation of the liver to pregnancy. Of note, considering that lipoprotein lipase activity in adipose tissue is reduced (29), the increased activity of malic enzyme in adipose tissue suggests that de novo lipogenesis accounts for the higher adiposity of pregnant rats. In fact, it has been

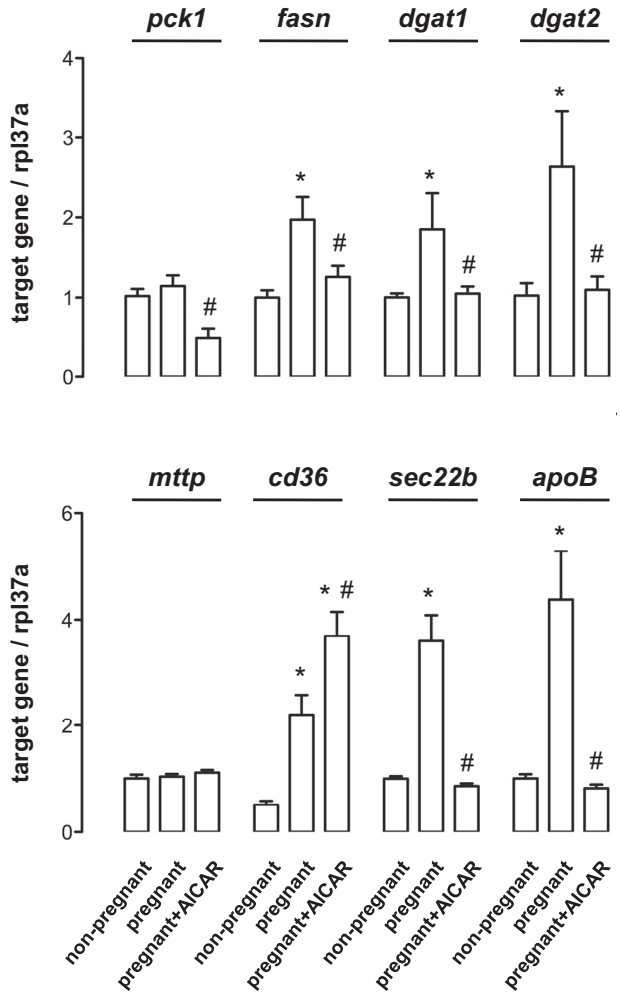

Fig. 7. Expression of genes related to TG synthesis and VLDL assembly and secretion in the liver from nonpregnant and pregnant rats treated or not with AICAR. Livers from nonpregnant and pregnant rats (*gestational day 19*), untreated or treated with AICAR, were processed for qPCR analysis of *pck1, fasn, dgat1*, and *dgat2* (*top*) and *mttp, cd36, sec22b*, and *apoB* (*bottom*). The results are shown as the means ± SE. *$P < 0.05$ vs. nonpregnant rats. #$P < 0.05$ vs. pregnant rats ($n = 4$ to 8).

demonstrated that lipogenesis was greater in adipose tissue from 19-day pregnant rats than nonpregnant rats (31).

Our data showing increased hepatic ACC and malic enzyme activities in conjunction with the increased expression of the *fasn* and *dgat* genes provide a molecular network that is able to support the adaptation of the liver to pregnancy. Indeed, previous research has observed reduced *fasn* and *dgat2* expression and reduced cellular content of FASN upon AMPK activation (47, 61). Given that we observed a restoration of hepatic TG content, as well as *fasn* and *dgat* expression, after increasing AMPK activity with AICAR treatment in pregnant rats, we next evaluated the expression of genes related to fatty acid transport and VLDL assembly.

The vesicle-trafficking protein homolog B Sec22b is one of the components of the SNARE (soluble *N*-ethylmaleimide-sensitive factor-attachment protein receptor) complex that is required for the delivery of VLDL-transport vesicles to the Golgi (56). Although the exportation of nascent VLDL particles to the Golgi is considered a physiologically highly regulated event, to our knowledge, there have been no previous demonstrations of the modulation of *sec22b* expression in a physiological model of an increased hepatic metabolic state. We observed that hepatic *sec22b* is upregulated in late pregnancy in an AMPK-dependent fashion, and treatment with AICAR restored its levels to those of a nonpregnant state. Likewise, the expression of *apoB*, the gene that encodes the essential structural VLDL protein apoB (the rat counterpart of the human apoB100), paralleled the changes in *sec22b* expression. Interestingly, proteomic studies have demonstrated that Sec22b binds to apoB100 at the ER level (48, 51). The same expression pattern of these two main proteins associated with nascent VLDL showed herein points to a mechanistic role for AMPK in VLDL biogenesis, intracellular trafficking, and secretion from the liver.

Consistent with the increased TG synthesis and VLDL secretion already described in late pregnancy (29, 37), our data show that the expression of fatty acid translocase (FAT)/CD36—the most important protein implicated in fatty acid uptake by skeletal muscle cells, cardiomyocytes, and adipocytes (9)—is increased in the livers of pregnant rats. *Cd36* expression is very low in healthy livers, suggesting that fatty acid uptake is FAT/CD36-independent under physiological conditions (38). However, in cardiac myocytes and perfused hearts, the prolonged AMPK activation by AICAR treatment increased the expression and the plasmalemmal content of FAT/CD36 (20). In accordance with the observations in heart tissue, we found that AICAR treatment increased hepatic *cd36* expression.

Notably, the above scenario, although consistent with the hypothesis of the central role of the AMPK pathway in the regulation of maternal hepatic fuel metabolism, requires further investigation. For example, we do not have data to explain the unexpectedly high expression of *cd36* in the livers of pregnant rats, even in the presence of low AMPK activity. As of now, we can only speculate that a combination of factors that constitute the complex internal milieu of pregnancy may be inducing the hepatic phenotype described herein. For example, the high insulin levels of late pregnancy could counteract the reduced AMPK activity and increase hepatic *cd36* expression (12).

Perspectives and Significance

Our data support the premise that AMPK participates in the regulation of maternal hepatic lipid metabolism. We suggest that the reduced hepatic AMPK activity of late pregnancy is likely to result in an increase in hepatic fatty acid synthesis that parallels a robust upregulation of VLDL assembly and secretion, thus manifesting as the reduced hepatic content of TG. This intracellular pathway is likely to be specific for the liver because the lipogenic activity of the adipose tissue was insensitive to AICAR. The transcriptional profile downstream of AMPK most likely encompasses the regulation of hepatic *dgat*, *fasn*, *sec22b*, and *apoB* expression.

ACKNOWLEDGMENTS

The authors would like to thank Dr. Rui Curi and Dr. Fabio Bessa Lima (University of Sao Paulo) for kindly allowing the use of facilities from their laboratories.

GRANTS

This study was supported by the Research Foundation of the State of São Paulo and National Council of Research.

DISCLOSURES

No conflicts of interest, financial or otherwise, are declared by the authors.

AUTHOR CONTRIBUTIONS

Author contributions: S.C.R., T.C.N., G.G.A., R.T.N., F.L.T.-L., C.L.-S., G.F.A., and S.B. conception and design of research; S.C.R., L.C.P., T.C.N., P.R.G., G.G.A., R.T.N., F.L.T.-L., L.C.C., and C.L.-S. performed experiments; S.C.R., L.C.P., T.C.N., P.R.G., G.G.A., R.T.N., F.L.T.-L., L.C.C., C.L.-S., G.F.A., and S.B. analyzed data; S.C.R., L.C.P., T.C.N., P.R.G., G.G.A., R.T.N., F.L.T.-L., L.C.C., C.L.-S., G.F.A., and S.B. interpreted results of experiments; S.C.R. and S.B. prepared figures; S.C.R., L.C.P., T.C.N., P.R.G., G.G.A., R.T.N., F.L.T.-L., L.C.C., C.L.-S., G.F.A., and S.B. approved final version of manuscript; G.F.A. and S.B. drafted manuscript; G.F.A. and S.B. edited and revised manuscript.

REFERENCES

1. **Al-Dwairi A, Pabona JM, Simmen RC, Simmen FA.** Cytosolic malic enzyme 1 (ME1) mediates high fat diet-induced adiposity, endocrine profile, and gastrointestinal tract proliferation-associated biomarkers in male mice. *PLoS One* 7: e46716, 2012.
2. **Anhê GF, Hirabara SM, Turrer TC, Caperuto LC, Anhê FF, Ribeiro LM, Marçal AC, Carvalho CR, Curi R, Machado UF, Bordin S.** Postpartum glycemic homeostasis in early lactating rats is accompanied by transient and specific increase of soleus insulin response through IRS2/AKT pathway. *Am J Physiol Regul Integr Comp Physiol* 292: R2225–R2233, 2007.
3. **Anhê GF, Nogueira TCA, Nicoletti-Carvalho JE, Lellis-Santos C, Barbosa HC, Cipolla-Neto J, Bosqueiro JR, Boschero AC, Bordin S.** Signal transducer and activator of transcription 3-regulated sarcoendoplasmic reticulum Ca^{2+}-ATPase 2 expression by prolactin and glucocorticoids is involved in the adaptation of insulin secretory response during the peripartum period. *J Endocrinol* 195: 17–27, 2007.
4. **Assifi MM, Suchankova G, Constant S, Prentki M, Saha AK, Ruderman NB.** AMP-activated protein kinase and coordination of hepatic fatty acid metabolism of starved/carbohydrate-refed rats. *Am J Physiol Endocrinol Metab* 289: E794–E800, 2005.
5. **Augustine RA, Ladyman SR, Grattan DR.** From feeding one to feeding many: hormone-induced changes in bodyweight homeostasis during pregnancy. *J Physiol* 586: 387–397, 2008.
6. **Berglund ED, Kang L, Lee-Young RS, Hasenour CM, Lustig DG, Lynes SE, Donahue EP, Swift LL, Charron MJ, Wasserman DH.** Glucagon and lipid interactions in the regulation of hepatic AMPK signaling and expression of PPARα and FGF21 transcripts in vivo. *Am J Physiol Endocrinol Metab* 299: E607–E614, 2010.
7. **Berglund ED, Lee-Young RS, Lustig DG, Lynes SE, Donahue EP, Camacho RC, Meredith ME, Magnuson MA, Charron MJ, Wasserman DH.** Hepatic energy state is regulated by glucagon receptor signaling in mice. *J Clin Invest* 119: 2412–2422, 2009.
8. **Berglund ED, Lustig DG, Baheza RA, Hasenour CM, Lee-Young RS, Donahue EP, Lynes SE, Swift LL, Charron MJ, Damon BM, Wasserman DH.** Hepatic glucagon action is essential for exercise-induced reversal of mouse fatty liver. *Diabetes* 60: 2720–2729, 2011.
9. **Bonen A, Chabowski A, Luiken JJ, Glatz JF.** Is membrane transport of FFA mediated by lipid, protein, or both? Mechanisms and regulation of protein-mediated cellular fatty acid uptake: molecular, biochemical, and physiological evidence. *Physiology (Bethesda)* 22: 15–29, 2007.
10. **Bravard A, Vial G, Chauvin MA, Rouillé Y, Bailleul B, Vidal H, Rieusset J.** FTO contributes to hepatic metabolism regulation through regulation of leptin action and STAT3 signalling in liver. *Cell Commun Signal* 12: 4, 2014.
11. **Bromati CR, Lellis-Santos C, Yamanaka TS, Nogueira TCA, Leonelli M, Caperuto LC, Gorjão R, Leite AR, Anhe GF, Bordin S.** UPR induces transient burst of apoptosis in islets of early lactating rats through reduced AKT phosphorylation via ATF4/CHOP stimulation of TRB3 expression. *Am J Physiol Regul Integr Comp Physiol* 300: R92–R100, 2011.
12. **Buqué X, Cano A, Miquilena-Colina ME, García-Monzón C, Ochoa B, Aspichueta P.** High insulin levels are required for FAT/CD36 plasma membrane translocation and enhanced fatty acid uptake in obese Zucker rat hepatocytes. *Am J Physiol Endocrinol Metab* 303: E504–E514, 2012.
13. **Burnol AF, Leturque A, Ferre P, Girard J.** Glucose metabolism during lactation in the rat: quantitative and regulatory aspects. *Am J Physiol Endocrinol Metab* 245: E351–E358, 1983.
14. **Butte NF.** Carbohydrate and lipid metabolism in pregnancy: normal compared with gestational diabetes mellitus. *Am J Clin Nutr* 71: 1256S–1261S, 2000.
15. **Camacho RC, Donahue EP, James FD, Berglund ED, Wasserman DH.** Energy state of the liver during short-term and exhaustive exercise in C57BL/6J mice. *Am J Physiol Endocrinol Metab* 290: E405–E408, 2006.
16. **Canniff KM, Smith MS, Lacy DB, Williams PE, Moore MC.** Glucagon secretion and autonomic signaling during hypoglycemia in late pregnancy. *Am J Physiol Regul Integr Comp Physiol* 291: R788–R795, 2006.
17. **Cansby E, Nerstedt A, Amrutkar M, Durán EN, Smith U, Mahlapuu M.** Partial hepatic resistance to IL-6-induced inflammation develops in type 2 diabetic mice, while the anti-inflammatory effect of AMPK is maintained. *Mol Cell Endocrinol* 393: 143–151, 2014.
18. **Carlson CL, Winder WW.** Liver AMP-activated protein kinase and acetyl-CoA carboxylase during and after exercise. *J Appl Physiol* 86: 669–674, 1999.
19. **Catalano PM, Huston L, Amini SB, Kalhan SC.** Longitudinal changes in glucose metabolism during pregnancy in obese women with normal glucose tolerance and gestational diabetes mellitus. *Am J Obstet Gynecol* 180: 903–916, 1999.
20. **Chabowski A, Momken I, Coort SL, Calles-Escandon J, Tandon NN, Glatz JF, Luiken JJ, Bonen A.** Prolonged AMPK activation increases the expression of fatty acid transporters in cardiac myocytes and perfused hearts. *Mol Cell Biochem* 288: 201–212, 2006.
21. **Chimin P, Farias TD, Torres-Leal FL, Bolsoni-Lopes A, Campaña AB, Andreotti S, Lima FB.** Chronic glucocorticoid treatment enhances lipogenic activity in visceral adipocytes of male Wistar rats. *Acta Physiol (Oxf)* 21: 409–420, 2014.
22. **Cole LK, Jacobs RL, Vance DE.** Tamoxifen induces triacylglycerol accumulation in the mouse liver by activation of fatty acid synthesis. *Hepatology* 52: 1258–1265, 2010.
23. **Connolly CC, Papa T, Smith MS, Lacy DB, Williams PE, Moore MC.** Hepatic and muscle insulin action during late pregnancy in the dog. *Am J Physiol Regul Integr Comp Physiol* 292: R447–R452, 2007.
24. **Faria JA, Kinote A, Ignacio-Souza LM, de Araújo TM, Razolli DS, Doneda DL, Paschoal LB, Lellis-Santos C, Bertolini GL, Velloso LA, Bordin S, Anhê GF.** Melatonin acts through MT1/MT2 receptors to activate hypothalamic Akt and suppress hepatic gluconeogenesis in rats. *Am J Physiol Endocrinol Metab* 305: E230–E242, 2013.
25. **González C, Alonso A, Fernández R, Patterson AM.** Regulation of insulin receptor substrate-1 in the liver, skeletal muscle and adipose tissue of rats throughout pregnancy. *Gynecol Endocrinol* 17: 187–197, 2003.
26. **Hasenour CM, Berglund ED, Wasserman DH.** Emerging role of AMP-activated protein kinase in endocrine control of metabolism in the liver. *Mol Cell Endocrinol* 366: 152–162, 2013.
27. **Henin N, Vincent MF, Gruber HE, Van den Berghe G.** Inhibition of fatty acid and cholesterol synthesis by stimulation of AMP-activated protein kinase. *FASEB J* 9: 541–546, 1995.
28. **Herrera E.** Metabolic adaptations in pregnancy and their implications for the availability of substrates to the fetus. *Eur J Clin Nutr* 54: S47–S51, 2000.
29. **Herrera E, Lasunción MA, Gomez-Coronado D, Aranda P, López-Luna P, Maier I.** Role of lipoprotein lipase activity on lipoprotein metabolism and the fate of circulating triglycerides in pregnancy. *Am J Obstet Gynecol* 158: 1575–1583, 1988.
30. **Imai K, Inukai K, Ikegami Y, Awata T, Katayama S.** LKB1, an upstream AMPK kinase, regulates glucose and lipid metabolism in cultured liver and muscle cells. *Biochem Biophys Res Commun* 351: 595–601, 2006.
31. **Knopp RH, Herrera E, Freinkel N.** Carbohydrate metabolism in pregnancy. 8. Metabolism of adipose tissue isolated from fed and fasted pregnant rats during late gestation. *J Clin Invest* 49: 1438–1446, 1970.
32. **Lellis-Santos C, Sakamoto LH, Bromati CR, Nogueira TCA, Leite AR, Yamanaka TS, Kinote A, Anhe GF, Bordin S.** The regulation of Rasd1 expression by glucocorticoids and prolactin controls peripartum maternal insulin secretion. *Endocrinology* 153: 3668–3678, 2012.
33. **Leturque A, Ferre P, Burnol AF, Kande J, Maulard P, Girard J.** Glucose utilization rates and insulin sensitivity in vivo in tissues of virgin and pregnant rats. *Diabetes* 35: 172–177, 1986.

34. **Liang CP, Tall AR.** Transcriptional profiling reveals global defects in energy metabolism, lipoprotein, and bile acid synthesis and transport with reversal by leptin treatment in *ob/ob* mouse liver. *J Biol Chem* 276: 49066–49076, 2001.
35. **Li H, Lee J, He C, Zou MH, Xie Z.** Suppression of the mTORC1/STAT3/Notch1 pathway by activated AMPK prevents hepatic insulin resistance induced by excess amino acids. *Am J Physiol Endocrinol Metab* 306: E197–E209, 2014.
36. **Lochhead PA, Salt IP, Walker KS, Hardie DG, Sutherland C.** 5-aminoimidazole-4-carboxamide riboside mimics the effects of insulin on the expression of the 2 key gluconeogenic genes PEPCK and glucose-6-phosphatase. *Diabetes* 49: 896–903, 2000.
37. **Lorenzo M, Caldés T, Benito M, Medina JM.** Lipogenesis in vivo in maternal and foetal tissues during late gestation in the rat. *Biochem J* 198: 425–842, 1981.
38. **Luiken JJ, Arumugam Y, Bell RC, Calles-Escandon J, Tandon NN, Glatz JF, Bonen A.** Changes in fatty acid transport and transporters are related to the severity of insulin deficiency. *Am J Physiol Endocrinol Metab* 283: E612–E621, 2002.
39. **Magkos F, Patterson BW, Mittendorfer B.** No effect of menstrual cycle phase on basal very-low-density lipoprotein triglyceride and apolipoprotein B-100 kinetics. *Am J Physiol Endocrinol Metab* 291: E1243–E1249, 2006.
40. **Martínez C, Ruiz P, Andrés A, Satrústegui J, Carrascosa JM.** Tyrosine kinase activity of liver insulin receptor is inhibited in rats at term gestation. *Biochem J* 263: 267–272, 1989.
41. **Munday MR, Milic MR, Takhar S, Holness MJ, Sugden MC.** The short-term regulation of hepatic acetyl-CoA carboxylase during starvation and refeeding in the rat. *Biochem J* 280: 733–737, 1991.
42. **Nerstedt A, Cansby E, Amrutkar M, Smith U, Mahlapuu M.** Pharmacological activation of AMPK suppresses inflammatory response evoked by IL-6 signalling in mouse liver and in human hepatocytes. *Mol Cell Endocrinol* 375: 68–78, 2013.
43. **Newham AP, Krieger K, Maly IP, Sasse D.** Changes in activity and intra-acinar distribution of glucose-6-phosphate dehydrogenase and malic enzyme during pregnancy in rat liver. *Histochemistry* 95: 365–371, 1991.
44. **Nicoletti-Carvalho JE, Lellis-Santos C, Yamanaka TS, Nogueira TC, Caperuto LC, Leite AR, Anhe GF, Bordin S.** MKP-1 mediates glucocorticoid-induced ERK1/2 dephosphorylation and reduction in pancreatic b-cell proliferation in islets from early lactating mothers. *Am J Physiol Endocrinol Metab* 299: E1006–E1015, 2010.
45. **Nogueira TC, Lellis-Santos C, Jesus DS, Taneda M, Rodrigues SC, Amaral FG, Lopes AM, Cipolla-Neto J, Bordin S, Anhê GF.** Absence of melatonin induces night-time hepatic insulin resistance and increased gluconeogenesis due to stimulation of nocturnal unfolded protein response. *Endocrinology* 152: 1253–1263, 2011.
46. **Ohira M1, Miyashita Y, Murano T, Watanabe F, Shirai K.** Metformin promotes induction of lipoprotein lipase in skeletal muscle through activation of adenosine monophosphate-activated protein kinase. *Metabolism* 58: 1408–1414, 2009.
47. **Oliveras-Ferraros C, Vazquez-Martin A, Fernández-Real JM, Menendez JA.** AMPK-sensed cellular energy state regulates the release of extracellular fatty acid synthase. *Biochem Biophys Res Commun* 378: 488–493, 2009.
48. **Rahim A, Nafi-valencia E, Siddiqi S, Basha R, Runyon CC, Siddiqi SA.** Proteomic analysis of the very low density lipoprotein (VLDL) transport vesicles. *J Proteomics* 75: 2225–2235, 2012.
49. **Ramadoss P, Unger-Smith NE, Lam FS, Hollenberg AN.** STAT3 targets the regulatory regions of gluconeogenic genes in vivo. *Mol Endocrinol* 23: 827–837, 2009.
50. **Ram PA, Park SH, Choi HK, Waxman DJ.** Growth hormone activation of Stat 1, Stat 3, and Stat 5 in rat liver. Differential kinetics of hormone desensitization and growth hormone stimulation of both tyrosine phosphorylation and serine/threonine phosphorylation. *J Biol Chem* 271: 5929–5940, 1996.
51. **Rashid KA, Hevi S, Chen Y, Le Caherec F, Chuck SL.** A proteomic approach identifies proteins in hepatocytes that bind nascent apolipoproteins B. *J Biol Chem* 277: 22010–22017, 2002.
52. **Rossi G, Sherwin RS, Penzias AS, Lapaczewski P, Jacob RJ, Shulman GI, Diamond MP.** Temporal changes in insulin resistance and secretion in 24-h-fasted conscious pregnant rats. *Am J Physiol Endocrinol Metab* 265: E845–E851, 1993.
53. **Schmoll D, Wasner C, Hinds CJ, Allan BB, Walther R, Burchell A.** Identification of a cAMP response element within the glucose- 6-phosphatase hydrolytic subunit gene promoter which is involved in the transcriptional regulation by cAMP and glucocorticoids in H4IIE hepatoma cells. *Biochem J* 338: 457–463, 1999.
54. **Seibert CS, Santoro ML, Tambourgi DV, Sampaio SC, Takahashi HK, Peres CM, Curi R, Sano-Martins IS.** *Lonomia obliqua* (Lepidoptera, Saturniidae) caterpillar bristle extract induces direct lysis by cleaving erythrocyte membrane glycoproteins. *Toxicon* 55: 1323–1330, 2010.
55. **Shaw RJ, Lamia KA, Vasquez D, Koo SH, Bardeesy N, Depinho RA, Montminy M, Cantley LC.** The kinase LKB1 mediates glucose homeostasis in liver and therapeutic effects of metformin. *Science* 310: 1642–1646, 2005.
56. **Siddiqi S, Mani AM, Siddiqi SA.** The identification of the SNARE complex required for the fusion of VLDL-transport vesicle with hepatic *cis*-Golgi. *Biochem J* 429: 391–401, 2010.
57. **Sim AT, Hardie DG.** The low activity of acetyl-CoA carboxylase in basal and glucagon stimulated hepatocytes is due to phosphorylation by AMP-activated protein kinase and not cyclic AMP-dependent protein kinase. *FEBS Lett* 233: 294–298, 1988.
58. **Wang H, Lafdil F, Kong X, Gao B.** Signal transducer and activator of transcription 3 in liver diseases: a novel therapeutic target. *Int J Biol Sci* 7: 536–550, 2011.
59. **Weigt C, Hertrampf T, Kluxen FM, Flenker U, Hülsemann F, Fritzemeier KH, Diel P.** Molecular effects of ER α- and β-selective agonists on regulation of energy homeostasis in obese female Wistar rats. *Mol Cell Endocrinol* 377: 147–158, 2013.
60. **Witters LA, Gao G, Kemp BE, Quistorff B.** Hepatic 5′-AMP-activated protein kinase: zonal distribution and relationship to acetyl-coA carboxylase activity in varying nutritional states. *Arch Biochem Biophys* 308: 413–419, 1994.
61. **Zhou G, Myers R, Li Y, Chen Y, Shen X, Fenyk-Melody J, Wu M, Ventre J, Doebber T, Fujii N, Musi N, Hirshman MF, Goodyear LJ, Moller DE.** Role of AMP-activated protein kinase in mechanism of metformin action. *J Clin Invest* 108: 1167–1174, 2001.